Unveiling quantum-limited operation of interband cascade lasers

Simone Borri (iD), Mario Siciliani de Cumis (iD), Silvia Viciani (iD), Francesco D'Amato (iD), and Paolo De Natale (iD)

open access

View Online   Export Citation   CrossMark

ARTICLES YOU MAY BE INTERESTED IN

One-dimensional, surface emitting, disordered Terahertz lasers
APL Photonics **5**, 036102 (2020); https://doi.org/10.1063/1.5131253

Diamond Brillouin laser in the visible
APL Photonics **5**, 031301 (2020); https://doi.org/10.1063/1.5134907

Ultra-broadband mid-infrared Ge-on-Si waveguide polarization rotator
APL Photonics **5**, 026102 (2020); https://doi.org/10.1063/1.5134973

AVS Quantum Science

SPECIAL ISSUE:
Quantum Sensing and Metrology

SUBMIT TODAY!

Co-Published by
AIP Publishing / AVS

AIP Publishing

Unveiling quantum-limited operation of interband cascade lasers

View Online   Export Citation   CrossMark

Simone Borri,[1,2,a] (ID) Mario Siciliani de Cumis,[1,3,b] (ID) Silvia Viciani,[1] (ID) Francesco D'Amato,[1] (ID) and Paolo De Natale[1,2] (ID)

AFFILIATIONS

[1] CNR-INO - Istituto Nazionale di Ottica, Largo E. Fermi 6, 50125 Firenze, Italy and LENS, via N. Carrara 1, 50019 Sesto Fiorentino, FI, Italy
[2] INFN, Sezione di Firenze, 50019 Sesto Fiorentino, FI, Italy
[3] ASI Agenzia Spaziale Italiana - Centro di Geodesia Spaziale, Località Terlecchia, 75100 Matera, Italy

[a] E-mail: simone.borri@ino.cnr.it
[b] Author to whom correspondence should be addressed: mario.sicilianidecumis@asi.it

ABSTRACT

A comprehensive experimental analysis of the frequency fluctuations of a mid-infrared interband cascade laser, down to the quantum-limited operation, is reported. These lasers differ from any other class of semiconductor lasers in their structure and internal carrier generation and transport processes. Although already commercially available, a full evaluation of their potential has not been possible, until now, mainly because their internal dynamics are not yet understood well enough. The measured intrinsic linewidth, down to 10 kHz, ranks them in between quantum cascade and bipolar semiconductor lasers. Understanding the noise features is especially important for demanding applications and is a necessary step for a deeper knowledge of the physical behavior for this class of lasers, in view of the development of novel designs for improved performance.

INTRODUCTION

Laser technology in the infrared (IR) spectral window is undergoing a major development, pushed by an increasing number of applications. In the last two decades from their appearance, quantum cascade and interband cascade lasers (QCLs and ICLs) have played a prominent role, relying on highly reliable, compact, low power consumption, semiconductor technology. Demonstrated in 1994,[1] QCLs are now a mature and commercial technology.[2] Their multi-watt output power emission and continuous wave and room temperature operation across the mid-IR, with an ~4–25 μm spectral coverage, have enabled their application in a broad range of fields.[3–6]

During the last two decades, QCLs gained considerable interest from both applied and fundamental physics viewpoints and nowadays have achieved a real impact on a large variety of technological applications. Their appealing and peculiar features are due to their intersubband operation, which, however, is responsible for their two main limitations, as well. First, their operation is limited to long wavelengths with a short-wave boundary around 4 μm due to limits in the maximum depth of the quantum wells. The second limitation is related to the very fast phonon relaxation process, which leads to a very short (~ps) upper lasing level lifetime, and is responsible for the high threshold current densities (typically >1 kA/cm^2) of these devices.

Invented in 1994,[7] and experimentally demonstrated in 1997,[8] ICLs are emerging as a valid alternative to IR sources in the 3–6 μm wavelength region. Their structure presents similarities and differences with respect to both standard bipolar semiconductor lasers and QCLs. ICLs utilize optical transitions between engineered energy levels in quantum wells, and laser emission occurs between an electron state in the conduction band and a hole state in the valence band. Moreover, they take advantage of a cascading mechanism over repeated active regions, which allows us to boost the quantum efficiency and, thus, the emitted optical power. As compared to QCLs, ICLs have the advantage of much longer lifetimes

(~1 ns) due to their interband transitions.[9,10] This allows us to circumvent the fast phonon scattering loss of intersubband devices such as QCLs and makes these devices much less demanding in terms of power consumption with lower compliance voltages and operating currents, still preserving a considerable available optical power (typically from few mW to tens of mW), which is particularly advantageous for in-field sensing. ICLs can also emit in the 3–4 μm window, where QCL operation is hard to achieve and important molecular bands for life science and astrophysics, e.g., the O–H and C–H stretching bands, can be found.[11] Although their use is constantly growing, especially for sensing applications,[12,13] and also steps toward improved design and materials with better performance have been made,[9,10] a full exploitation of ICLs' potential has not been possible, thus far, because of an inadequate understanding of their internal physics. Indeed, the carrier generation and transport mechanisms of ICLs significantly differ from those of conventional diode lasers and QCLs. QCLs are unipolar devices, all the carriers are externally injected, and the internal current flow is entirely due to electrons passing through repeated quantum well structures. In diode lasers, instead, all the electrons and holes are injected into the conduction and valence bands, respectively, from the two contacts. On the contrary, ICLs are the only known lasers in which electrons and holes are generated internally at semi-metallic interfaces produced by an applied bias voltage.[10] Moreover, as the generated carriers are dragged away, in opposite directions, by the external electric field, equal numbers of electrons and holes are continuously regenerated at the semi-metallic interfaces to maintain the thermal quasi-equilibrium condition.[10] This behavior, which still requires a comprehensive modeling, reflects in the frequency noise characteristics of these lasers and is expected to set similarities and differences with respect to QCLs and diode lasers.

Up to now, only a few issues about frequency dynamics of these devices, including the α linewidth enhancement factor and photon noise, have been addressed,[14–17] but no modeling of carrier generation and transport processes has been reported yet, as well as no experimental investigation of their frequency noise characteristics has been published. If we look back over what happened in recent years for QCLs, we see that understanding their frequency noise features[18–22] allowed us to test specific models,[23] triggered a series of improvements in the stabilization of the QCL chip temperature and driving current, and boosted the development of frequency/phase stabilization techniques. This led to spectacular linewidth narrowing,[24–27] allowing for record sensitivities in trace-gas detection, down to the ppq level,[28] and enabling sophisticated precision spectroscopy experiments.[4,29,30] Just as it happened for QCLs, a fundamental step toward comprehensive modeling and optimized design of ICLs can be achieved by a complete experimental analysis of their frequency noise features and internal dynamics.

In this paper, we show that ICLs have an intrinsic linewidth intermediate between the semiconductor lasers with the lowest phase noise, i.e., QCLs, and bipolar lasers such as quantum-well and vertical-cavity emitting devices. In particular, a comprehensive experimental investigation of the frequency noise power spectral density (FNPSD) of a commercial ICL emitting at 4.6 μm is reported. To this purpose, a set of precise requirements has to be fulfilled, especially when the goal is to unveil the small quantum-limited contributions of intrinsic frequency noise. Generally, this is not a trivial operation to perform and can become very challenging in spectral

regions such as the mid-IR, where optical and optoelectronic components are not as good as those available for shorter wavelengths. First of all, the laser has to be supplied with an ultra-low-noise current driver, else the tiny frequency noise level associated with spontaneous emission is completely surmounted by the contribution from current noise or from laser intensity fluctuations. Then, a fast and sensitive photodiode is required, along with a high performance spectrum analyzer, to explore all the significant regions of noise spectrum, from the low-frequency region, where flicker noise dominates, up to Fourier frequencies of tens of MHz, where the noise spectrum flattens to a white noise contribution. In our work, the dependence of the noise spectrum on laser operating current and temperature is shown, which can be of particular interest for the development of a model of internal dynamics. The analysis allows us to highlight the main frequency noise contributions in ICLs, showing similarities and differences with respect to standard diode lasers and to QCLs, and to measure intrinsic linewidths at different power levels, down to the 10-kHz level.

FREQUENCY NOISE MEASUREMENTS

The laser used in this experiment is a room-temperature distributed feedback (DFB) ICL emitting around 4.6 μm from Nanoplus. We operated the laser from 14.5 °C to 38 °C with driving currents from ~35 mA to ~80 mA, measuring a maximum emitted power of ~4 mW. The ICL was supplied by an ultra-low-noise QubeCL current driver from ppqSense. In order to avoid parasitic optical feedback onto the laser, optical isolation was achieved with a polarizer combined to a quarter-wave plate. For frequency noise measurements, the slope of a strong molecular absorption line was used to convert frequency fluctuations into amplitude fluctuations that were detected by using a thermoelectrically cooled HgCdTe detector from VIGO (PVI-4TE-6, DC-200 MHz). The frequency response of the detector is flat up to about 100 MHz. A DC-coupled spectrum analyzer was used to analyze and acquire the signal. More details on the ICL structure and characteristics and on the experimental setup can be found in the supplementary material.

In Fig. 1, the FNPSD of an ICL emitting at 4.6 μm and that of a room-temperature DFB QCL emitting at 4.3 μm are shown for a qualitative comparison. Apart from the different noise levels, which strongly depend on the operating temperature and current and, therefore, cannot be directly used to compare the two sources without a proper theoretical model, a simple analysis of the different trends of the spectra also allows us to understand the main effects contributing to the frequency noise for the two lasers. While a strong 1/f component dominates at low Fourier frequencies, the ICL noise spectrum shows a significant deviation from this trend in the 10–1000 kHz range, which is typical of bipolar semiconductor lasers. This is due to thermal effects with a cutoff at a few hundreds kHz (red line in Fig. 1). This is strongly suppressed in QCLs due to fast recombination processes.[20,23] Both noise spectra also show a flattening to a white noise above 1 MHz, with a strong difference in the noise level (more than two orders of magnitude), also due to the different Henry α-factor,[14] which takes into account additional broadening due to relaxation–oscillation noise, and which for QCLs is negligible. For all the acquired spectra, we checked that the contribution from amplitude noise maintains well below the overall
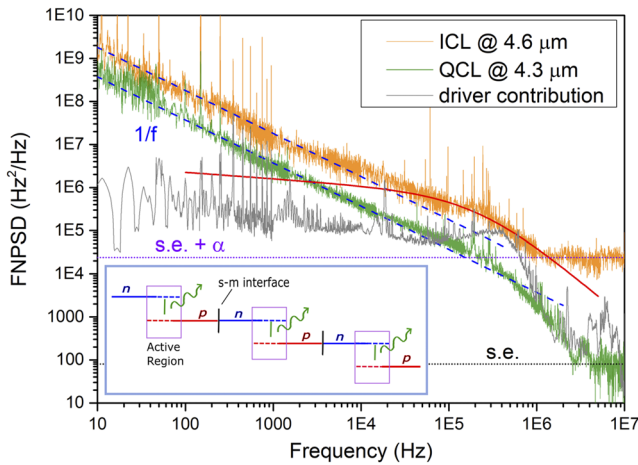
FIG. 1. The FNPSD of a DFB QCL at 4.3 μm and of an ICL at 4.6 μm is shown for qualitative comparison of their different trends. The QCL is operated at 15 °C and 750 mA with an output power of ~10 mW. The ICL is operated at 38 °C and 77 mA with an output power of ~0.5 mW. The main contributions to the noise trend are shown and discussed in the text (s.e. = spontaneous emission). The driver contribution to the ICL FNPSD is also shown (gray trace). Inset: schematic of the carrier generation process of an ICL.

FNPSD level at all Fourier frequencies. The measured current driver contribution to the ICL FNPSD is also shown in Fig. 1 in order to be sure that it does not represent, in any part of the spectrum, a limiting factor to the ICL frequency noise analysis.

Focusing on the ICL frequency noise, an extensive analysis has been carried out for different operating conditions of driving current and temperature. This analysis, which is fundamental for modeling the noise properties and inner dynamics of these devices, shows that different operating conditions sensibly modify the ICL FNPSD level in the low Fourier-frequency part, where technical noise dominates, as well as in the white-noise part. For the sake of clarity, these two interesting parts of the frequency noise spectrum have been separated and zoomed. In Fig. 2, the low frequency part of the FNPSD is shown in the range of 100–1000 Hz, where 1/f noise dominates. In Fig. 2(a), the different noise curves at the same operating current, I = 77 mA, are reported for different temperatures. Figure 2(b) reports the different noise spectra for different driving currents at the fixed temperature, T = 16.3 °C.

The data show that the 1/f component of the noise level increases monotonically with both current and temperature in a similar way to what happens to intensity noise.[21] This behavior is expected in bipolar lasers and corresponds to higher noise levels as both carrier density and mobility increase.

A similar analysis can be done for the high-frequency part of the frequency noise spectrum in order to study the dependence of the white-noise level on the operating point, as shown in Fig. 3. Here, the noise level increases with increasing temperature but behaves oppositely with current. This behavior can be understood if we keep in mind that the white noise level, N_w, of the FNPSD is proportional to the laser intrinsic linewidth, according to the simple formula[31]

$$\delta \nu = \pi N_w. \tag{1}$$
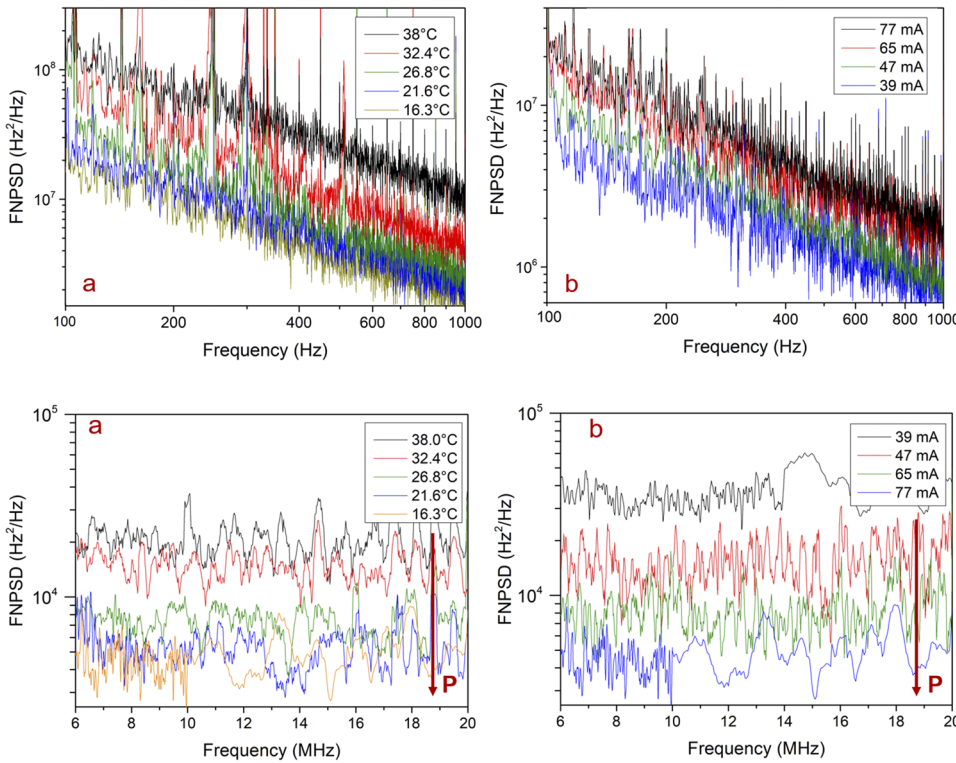
FIG. 2. FNPSD vs operating conditions, low-frequency part. The 1/f part of the ICL FNPSD is plotted as a function of (a) the operating temperature at a fixed current of 77 mA and (b) the driving current for a fixed temperature of 16.3 °C.

FIG. 3. FNPSD vs operating conditions, high-frequency part. The *white-noise* part of the ICL FNPSD is plotted as a function of (a) the operating temperature at a fixed current of 77 mA and (b) the driving current for the fixed temperature of 16.3 °C. The red arrows pointing downward show how the laser power grows for the different traces.
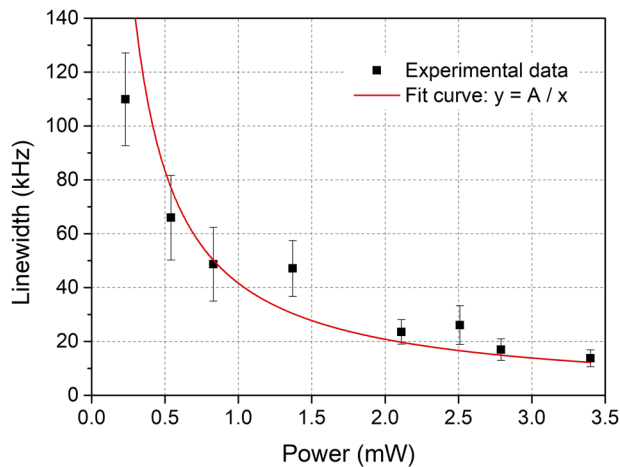
FIG. 4. The ICL intrinsic linewidth (FWHM) is plotted as a function of the output power. The graph shows all the different operating conditions studied in the experiment. Each point of the graph is obtained as the average value (and error bars as the *rms* values) of the data shown in Fig. 3 multiplied by π. The points have been fitted by a y = A/x function (red curve), according to the Schawlow–Townes formula [Eq. (2)].

This, according to frequency-noise theory,[31–33] represents the FWHM of the purely Lorentzian power spectrum associated with the spontaneous emission, enhanced by the Henry α factor. The general formula, given by the modified Schawlow–Townes theory, shows that the intrinsic linewidth is inversely proportional to the output optical power according to

$$\delta\nu = \frac{c^2 h\nu n_{sp}\alpha_{tot}\alpha_m}{4\pi n_g P}\left(1+\alpha^2\right),\tag{2}$$

where n_{sp} is the spontaneous emission factor, also called the population inversion factor, α_{tot} and α_m are the total losses in the cavity and the mirror losses, respectively, n_g is the group refractive index, and P is the output power.

The recorded noise spectra shown in Fig. 3 show this behavior, as the noise level decreases with increasing power. By averaging each of the curves in the white noise region, it is possible to estimate the ICL intrinsic linewidth for the different laser power levels, according to Eq. (1). The resulting data are shown in Fig. 4.

DISCUSSION

ICLs are expected to present similarities with respect to bipolar semiconductor lasers due to their interband operation. Nonetheless, their peculiar carrier generation and transport processes mark a substantial difference with other near and mid-infrared semiconductor lasers.

As shown in Fig. 1, the similarities with the behavior of diode lasers are clear, as well as the differences with unipolar devices such as QCLs. The noise spectrum presents a large technical noise contribution with a cutoff in the 100 kHz–1 MHz range, which can be attributed to thermal dynamics. The strong $1/f$ component of the spectrum largely depends on the operating conditions, showing

a monotonic trend with current and temperature. The behavior is similar to what was observed in intensity noise measurements,[15] suggesting a common explanation connected to internal carrier-density fluctuations. Indeed, ICLs, being bipolar semiconductor devices, are expected to present a number of recombination processes, radiative and not radiative, in which temperature, doping, and chemical potentials play a fundamental role. In particular, a possible hypothesis involves deep-level trap mechanisms responsible for generation–recombination noise, as those studied for quantum well lasers.[34] As is well known, $1/f$ noise can be attributed to many different physical mechanisms,[35] each leading to a different dependence on current. From our measurements, a linear/slightly parabolic trend is observed for the $1/f$ noise level vs current.

Following the general approach reported in Ref. 33 from a numerical integration of the FNPSD curve, we obtain a width of ~3 MHz (FWHM) over 1 s for the power spectrum of the laser. It is important to stress the fact that this value is strongly affected by current noise from the driver, similarly to what happens for QCLs, where the choice of a low-noise driver is essential for a more frequency-stable emission. Although technical noise represents, by far, the main contribution to the laser linewidth, its dependence on the operating conditions shows that it can be removed using proper locking mechanisms and feedback onto the driving current. This represents one of the next steps to fully exploit the potential of these lasers.

Above 1 MHz, the flat noise level shows an inverse proportionality relation with the optical power (Fig. 4). Here, both the measured amplitude and current noise contributions lay well below the recorded frequency noise level so that we can confidently attribute the measured noise to the white noise leading to the intrinsic linewidth [Eq. (1)]. The inverse proportionality with power is in agreement with the expected behavior according to the Schawlow–Townes formula [Eq. (2)]. A ~10 kHz intrinsic linewidth is obtained, which can be reached far from threshold, with a few mW of output power.

Differently from QCLs, for which the flat noise level is orders of magnitude lower, for ICLs, an important role is played by the Henry enhancement factor α, which typically ranges from 2 to 5 for near-IR quantum well lasers.[36] Starting from the general equation (2), we can give an estimation of the Henry α-factor for our ICL basing on our experimental measurements of the ICL intrinsic linewidth. As we do not have access to the actual internal parameters for our device, we have to base our estimation on the few data available in the literature for similar devices. In particular, we consider $\alpha_{tot} \approx 10$ cm^{-1} [10,37] and $n_g \approx 3.45$.[9] From the length and facet reflectivity of our device (see the supplementary material), we calculate $\alpha_m \approx 2$ cm^{-1}. The population inversion factor n_{sp} is generally considered between 1 and 2 for semiconductor lasers,[38,39] and we consider here $n_{sp} = 1.5$ according to the examples in Refs. 38 and 39. Considering the fitted linewidth of 13.8 kHz at P = 3 mW output power (Fig. 4), an α-factor of 2.1 is calculated from Eq. (2), in good agreement with the value of 2.2 recently measured for an ICL emitting at 3.39 μm.[14] It is interesting to note that, thanks to the same semiconductor material combination, the values of the ICLs' parameters are very similar to those of QCLs emitting in the same region with only a slightly higher internal loss parameter α_{tot}, probably due to a not yet optimized structure.

Our measured value for the ICL intrinsic linewidth can also be compared with the only previous estimation reported in Ref. 17,

where some frequency dynamics properties of a device emitting at 3.27 μm are measured using an interferometric technique. The values reported there are much higher (hundreds of kHz) than those we measured, and a behavior for the intrinsic linewidth vs driving current opposite to the expected one (linewidth increasing with current) was also found. This may suggest a large contribution from the driver current noise, affecting the measurements and preventing the right estimation of the intrinsic linewidth level. The values shown in Fig. 4 can be associated with those measured for semiconductor quantum well lasers and VCSELs,[40] for which intrinsic linewidths in the tens of kHz range are reported. This similarity, together with that connected to the 1/f noise part cited before and to the value of the Henry α-factor, can be a starting point for modeling ICLs' internal dynamics. Moreover, the strong dependence of the frequency noise on current and temperature suggests that a systematic study of other dynamic spectral characteristics (slope efficiency, tuning rates, frequency, and amplitude modulation factors) is required in order to compose the puzzle of these peculiar laser sources.

In conclusion, we are convinced that, in the framework of many areas of quantum technologies, and starting from the low-noise behavior unveiled in our work, ICLs can actually qualify as game-changing laser sources. Indeed, the unique combination of a tailorable, quantum-by-design band structure engineering and the high-generation efficiency could lead to squeezed, comb-emitting, disruptive radiation sources.

SUPPLEMENTARY MATERIAL

See the supplementary material for the details and characterization of the ICL and for description of the measurement method and setup.

AUTHOR'S CONTRIBUTIONS

S.B. contributed to the development of the setup, performed the noise measurements, analyzed the data, and wrote the manuscript; M.S.d.C. contributed to the development of the experiment, to the data analysis, and to the manuscript preparation; S.V. and F.D'A. contributed to the conception of the experiment and to the data interpretation and revised the manuscript; P.D.N. contributed to the conception of the experiment and coordinated the experiment.

ACKNOWLEDGMENTS

REFERENCES

[1]J. Faist, F. Capasso, D. L. Sivco, C. Sirtori, A. L. Hutchinson, and A. Y. Cho, "Quantum cascade lasers," Science **264**, 553–556 (1994).

[2]M. Vitiello, G. Scalari, B. Williams, and P. De Natale, "Quantum cascade lasers: 20 years of challenges," Opt. Express **23**, 5167–5182 (2015).

[3]M. Troccoli, J. Fan, G. Tsvid, and X. Wang, "High-performance quantum cascade lasers for industrial applications," in *The Wonder of Nanotechnology:*

Quantum Optoelectronic Devices and Applications, edited by M. Razeghi, L. Esaki, and K. von Klizing (SPIE, Bellingham, 2013), Chap. X.

[4]L. Consolino, F. Cappelli, M. Siciliani de Cumis, and P. De Natale, "QCL-based frequency metrology from the mid-infrared to the THz range: A review," Nanophotonics **8**, 181 (2018).

[5]A. Schwaighofer, M. Brandstetter, and B. Lendl, "Quantum cascade lasers (QCLs) in biomedical spectroscopy," Chem. Soc. Rev. **46**, 5903–5924 (2017).

[6]S. Viciani, A. Montori, A. Chiarugi, and F. D'Amato, "A portable quantum cascade laser spectrometer for atmospheric measurements of carbon monoxide," Sensors **18**, 2380 (2018).

[7]R. Q. Yang, "Infrared laser based on intersubband transitions in quantum wells," Superlattices Microstruct. **17**, 77–83 (1995).

[8]C. H. Lin, R. Q. Yang, D. Zhang, S. J. Murry, S. S. Pei, A. A. Allerman, and S. R. Kurtz, "Type-II interband quantum cascade laser at 3.8 μm," Electron. Lett. **33**, 598–599 (1997).

[9]I. Vurgaftman, R. Weih, M. Kamp, J. R. Meyer, C. L. Canedy, C. S. Kim, M. Kim, W. W. Bewley, C. D. Merritt, J. Abell, and S. Höfling, "Interband cascade lasers," J. Phys. D: Appl. Phys. **48**, 123001 (2015).

[10]I. Vurgaftman, W. W. Bewley, C. L. Canedy, C. S. Kim, M. Kim, C. D. Merritt, J. Abell, J. R. Lindle, and J. R. Meyer, "Rebalancing of internally generated carriers for mid-infrared interband cascade lasers with very low power consumption," Nat. Commun. **2**, 585 (2011).

[11]S. A. Sandford, L. J. Allamandola, A. G. G. M. Tielens, K. Sellgren, M. Tapia, and Y. Pendleton, "The interstellar C-H stretching band near 3.4 microns: Constraints on the composition of organic material in the diffuse interstellar medium," Astrophys. J. **371**, 607–620 (1991).

[12]G. Wysocki, Y. Bakhirkin, S. So, F. K. Tittel, C. J. Hill, R. Q. Yang, and M. P. Fraser, "Dual interband cascade laser based trace-gas sensor for environmental monitoring," Appl. Opt. **46**, 8202–8210 (2007).

[13]W. Ren, L. Luo, and F. K. Tittel, "Sensitive detection of formaldehyde using an interband cascade laser near 3.6 μm," Sens. Actuators, B **221**, 1062–1068 (2015).

[14]Y. Deng, B. B. Zhao, and C. Wang, "Linewidth broadening factor of an interband cascade laser," Appl. Phys. Lett. **115**, 181101 (2019).

[15]P. A. Folkes, "Interband cascade laser photon noise," J. Phys. D: Appl. Phys. **41**, 245109 (2008).

[16]J. Li, Z. Du, and Y. An, "Frequency modulation characteristics for interband cascade lasers emitting at 3 μm," Appl. Phys. B **121**, 7 (2015).

[17]Z. Du, G. Luo, Y. An, and J. Li, "Dynamic spectral characteristics measurement of DFB interband cascade laser under injection current tuning," Appl. Phys. Lett. **109**, 011903 (2016).

[18]S. Bartalini, S. Borri, P. Cancio Pastor, A. Castrillo, I. Galli, G. Giusfredi, D. Mazzotti, L. Gianfrani, and P. De Natale, "Observing the intrinsic linewidth of a quantum cascade laser: Beyond the Schawlow-Townes limit," Phys. Rev. Lett. **104**, 083904 (2010).

[19]S. Bartalini, S. Borri, I. Galli, G. Giusfredi, D. Mazzotti, T. Edamura, N. Akikusa, M. Yamanishi, and P. De Natale, "Measuring frequency noise and intrinsic linewidth of a room-temperature DFB quantum cascade laser," Opt. Express **19**, 17996 (2011).

[20]S. Borri, S. Bartalini, P. Cancio, I. Galli, G. Giusfredi, D. Mazzotti, M. Yamanishi, and P. De Natale, "Frequency-noise dynamics of mid-infrared quantum cascade lasers," IEEE J. Quantum Electron. **47**, 984 (2011).

[21]L. Tombez, S. Schilt, J. Di Francesco, T. Fuhrer, B. Rein, T. Walther, G. Di Domenico, D. Hofstetter, and P. Thomann, "Linewidth of a quantum-cascade laser assessed from its frequency noise spectrum and impact of the current driver," Appl. Phys. B **109**, 407 (2012).

[22]F. Mezzapesa, L. L. Columbo, M. Brambilla, M. Dabbicco, S. Borri, M. S. Vitiello, H. E. Beere, D. A. Ritchie, and G. Scamarcio, "Intrinsic stability of quantum cascade lasers against optical feedback," Opt. Express **21**, 13748 (2013).

[23]M. Yamanishi, T. Edamura, K. Fujita, N. Akikusa, and H. Kan, "Theory of the intrinsic linewidth of quantum cascade lasers: Hidden reason for the narrow linewidth and line-broadening by thermal photons," IEEE J. Quantum Electron. **44**, 12 (2008).

[24]F. Cappelli, I. Galli, S. Borri, G. Giusfredi, P. Cancio, D. Mazzotti, A. Montori, N. Akikusa, M. Yamanishi, S. Bartalini, and P. De Natale, "Subkilohertz linewidth

room-temperature mid-IR quantum cascade laser using a molecular sub-Doppler reference," Opt. Lett. **37**, 4811 (2012).

[25] L. Tombez, S. Schilt, D. Hofstetter, and T. Südmeyer, "Active linewidth-narrowing of a mid-infrared quantum cascade laser without optical reference," Opt. Lett. **38**, 5079 (2013).

[26] M. Siciliani de Cumis, S. Borri, G. Insero, I. Galli, A. Savchenkov, D. Eliyahu, V. Ilchenko, N. Akikusa, A. Matsko, L. Maleki, and P. De Natale, "Microcavity stabilized quantum cascade laser," Laser Photonics Rev. **10**, 153 (2016).

[27] B. Argence, B. Chanteau, O. Lopez, D. Nicolodi, M. Abgrall, C. Chardonnet, C. Daussy, B. Darquié, Y. Le Coq, and A. Amy-Klein, "Quantum cascade laser frequency stabilisation at the sub-Hz level," Nat. Photonics **9**, 456 (2015).

[28] I. Galli, S. Bartalini, R. Ballerini, M. Barucci, P. Cancio, M. De Pas, G. Giusfredi, D. Mazzotti, N. Akikusa, and P. De Natale, "Spectroscopic detection of radiocarbon dioxide at parts-per-quadrillion sensitivity," Optica **3**, 385 (2016).

[29] G. Insero, S. Borri, D. Calonico, P. Cancio, C. Clivati, D. D'Ambrosio, P. De Natale, M. Inguscio, F. Levi, and G. Santambrogio, "Measuring molecular frequencies in the 1-10 μm range at 11-digits accuracy," Sci. Rep. **7**, 12780 (2017).

[30] S. Borri, G. Insero, G. Santambrogio, D. Mazzotti, F. Cappelli, I. Galli, G. Galzerano, M. Marangoni, P. Laporta, V. Di Sarno, L. Santamaria, P. Maddaloni, and P. De Natale, "High-precision molecular spectroscopy in the mid-infrared using quantum cascade lasers," Appl. Phys. B **125**, 18 (2019).

[31] C. H. Henry, "Theory of linewidth of semiconductor lasers," IEEE J. Quantum Electron. **18**, 259 (1982).

[32] M. Zhu and J. L. Hall, "Stabilization of optical phase/frequency of a laser system: Application to a commercial dye laser with an external stabilizer," J. Opt. Soc. Am. B **10**, 802 (1993).

[33] D. S. Elliott, R. Roy, and S. J. Smith, "Extracavity laser band-shape and band-width modification," Phys. Rev. A **26**, 12 (1982).

[34] G. Hu, J. Li, and Y. Shi, "The g–r noise in quantum well semiconductor lasers and its relation with device reliability," Opt. Laser Technol. **39**, 165 (2007).

[35] F. N. Hooge, T. G. M. Kleipenning, and L. K. J. Vandamme, "Experimental studies on 1/f noise," Rep. Prog. Phys. **44**, 479 (1981).

[36] M. Lerttamrab, S. L. Chuang, R. Q. Yang, and C. J. Hill, "Linewidth enhancement factor of a type-II interband-cascade laser," J. Appl. Phys. **96**, 3568 (2004).

[37] M. Kim, W. W. Bewley, C. L. Canedy, C. Soo Kim, C. D. Merritt, J. Abell, I. Vurgaftman, and J. R. Meyer, "High-power continuous-wave interband cascade lasers with 10 active stages," Opt. Express **23**, 9664 (2015).

[38] L. A. Coldren, S. W. Corzine, and M. L. Mašanović, *Diode Lasers and Photonic Integrated Circuits*, 2nd ed. (John Wiley & Sons, 2012), Chap. 4.

[39] C. H. Henry, "Line broadening of semiconductor lasers," in *Coherence, Amplification, and Quantum Effects in Semiconductor Lasers*, edited by Y. Yamamoto (John Wiley & Sons, 1991).

[40] A. Laurain, M. Myara, G. Beaudoin, I. Sagnes, and A. Garnache, "Multiwatt–power highly–coherent compact single–frequency tunable vertical–external–cavity–surface–emitting–semiconductor–laser," Opt. Express **18**, 014627 (2010).

[41] R. Weih, L. Nähle, S. Höfling, J. Koeth, and M. Kamp, "Single mode interband cascade lasers based on lateral metal gratings," Appl. Phys. Lett. **105**, 071111 (2014).

[42] I. E. Gordon *et al.*, "The HITRAN2016 molecular spectroscopic database," J. Quant. Spectrosc. Radiat. Transfer **203**, 3 (2017).